2015 International Symposium on Nonlinear Theory and its Applications
NOLTA2015, Kowloon, Hong Kong, China, December 1-4, 2015

Linear response measurement of both a single and an array of cantilevers in a high amplitude nonlinear state

M. Sato†, Y. Sada†, S. Shige† and A. J. Sievers‡
†Graduate School of Natural Science and Technology, Kanazawa University
Kakumamachi, Kanazawa, Ishikawa 920-1192, Japan
‡Laboratory of Atomic and Solid State Physics, Cornell University
Ithaca, NY 14853-2501, USA
Email: msato153@staff.kanazawa-u.ac.jp

Abstract– As the bifurcation frequency for the single cantilever is approached the linear response measurement of the frequency shift and peak height of the natural frequency (NF) resonance, which corresponds to a homogeneous solution of a driven nonlinear equation of motion, is in good agreement with analytical calculations for a single Duffing resonator. Linear response measurements also provide information about the bifurcation mechanism for an intrinsic localized mode in a micro-cantilever array. We find that the most prominent structure in the linear response spectrum for the ILM is, again, the NF. When the measured NFs of the two geometrically different nonlinear systems are compared the results are very similar at large amplitudes, including the appearance of nonlinear damping, which grows with increased cantilever amplitude.

1. Introduction

Micromechanical systems have attracted much interest because of their useful applications and/or novel dynamical behavior. [1, 2] A cantilever array provides a platform where experiments on collective nonlinear behavior can be compared with theory. Intrinsic localized modes (ILMs) represent one novel property of the dynamical excitations of a nonlinear lattice.[3-5] ILMs can be generated and kept at steady state in the cantilever array by a continuous vibrational excitation, easily produced by a piezo-electric transducer (PZT) attached to the cantilever array. An ILM exhibits a bifurcation when the PZT frequency is changed beyond a stable region, or when a moveable impurity approaches an ILM and repulsion or attraction along the lattice take place. [6] A linear response measurement is a very powerful tool to investigate the mechanism behind such bifurcation dynamics.

Linear response is measured when a low level sinusoidal probe is applied to the ILM and a vibration response caused by this perturbation is measured as a spectrum by scanning the probe frequency. If some resonance peaks in the spectrum shift in frequency near the bifurcation point, we expect that those corresponding normal modes are connected to the transition. [7, 8] Peaks in the spectrum include a natural frequency (NF), linear local modes (LLMs) associated with the ILM [9], and band modes (BMs) of the lattice.

In this paper, we report on the NF measurement of a single micro-cantilever in a high amplitude state. Because of the driven-damped condition to maintain steady state, there should be one pair of peaks associated with the NF, symmetrically located about the pump frequency. We show that the measured NF results of a single Duffing resonator agree with those determined from analytical calculation or simulations and that these results also are similar at large amplitudes to those observed for the NF of an ILM in an array.

2. Experiments

Figure 1 is a schematic of the experimental setup for the linear response measurement. The micro-cantilever sample is set in a vacuum chamber with a piezo-electric driver (PZT). Two oscillators are connected to the PZT, one is the pump to maintain the nonlinear large amplitude state by a large AC signal, and the other is a probe for the spectrum measurement with a very small AC amplitude. A cantilever is 50 μm long, 15 μm width and 300 nm thick. The cantilever has a positive nonlinearity, that is, the spring constant becomes hard as the amplitude increases.

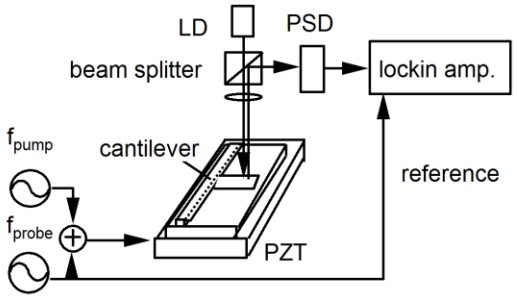

Fig. 1 Experimental setup for the linear response measurement. A cantilever is set in a vacuum chamber and driven vertically by a piezo-transducer (PZT). A laser diode (LD) , beam splitter, and position sensitive detector (PSD) are employed for the vibration measurement. Large amplitude oscillation at f_{pump} and weak amplitude oscillation at f_{prove} are induced in the cantilever. The response is analyzed with a lock-in amplifier.

To make the linear measurement, first, the pump frequency is increased from a frequency below the linear resonance frequency to one above so that the oscillator reaches a high amplitude state. Then, the probe frequency

is scanned across the pump frequency to obtain the required linear response spectrum. The probe signal is analyzed by a lock-in amplifier, which gives sine and cosine response when the cosine probe as used as a reference signal. Typical real and imaginary parts of the response curve are displayed in Fig. 2. The large central peak is due to the pump signal.

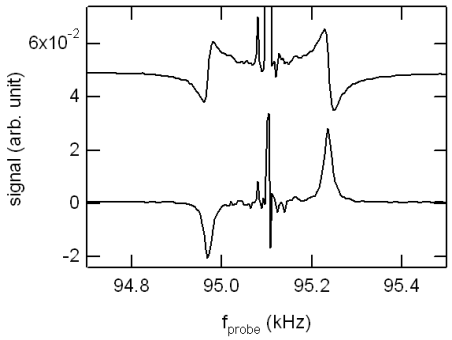

Fig. 2. Real (upper) and imaginary (lower) parts of the response curve vs probe frequency for the single cantilever in a high amplitude state. Sharp, large peak at 95.1 kHz is due to the large amplitude oscillation by the pump. Somewhat broader peaks symmetrically located about the pump frequency are the sideband responses. Pump amplitude is 0.41V and probe amplitude is 4.2mV.

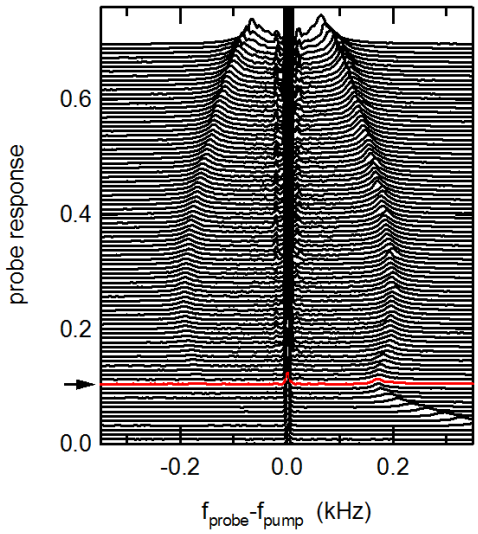

Fig. 3 Response spectra vs probe-pump difference frequency for various pump frequencies. PZT pump amplitude = 0.41V; probe amplitude = 4.2mV. Pump frequency ranges from 92.30 to 95.78 kHz in 0.04kHz increments. Arrow identifies the linear spectrum for $f_{pump} = 92.812\text{kHz}$.

Figure 3 presents the pump frequency dependence of the probe response. Spectra are ordered from bottom to top with increasing pump frequency. The arrow on the ordinate identifies that particular spectrum when the pump frequency coincides with the linear resonance frequency of the cantilever. Below this frequency there is only one resonance peak, on the right hand side; but as the pump frequency increases another resonance appears on the left hand side. This peak height increases with the increasing pump frequency and at first the NF gap frequency increases as well. Then at still larger frequencies it decreases.

The amplitude dependence of the cantilever vs pump frequency, as well as the gap frequency and the peak height of the NF are summarized in Fig. 4. The amplitude responses for various pump excitation levels are presented in Fig. 4(a). Figures 4(b) and (c) show the gap frequency and NF peak height dependences, respectively. The gap frequency decreases as the pump frequency approaches the upper bifurcation point, while the peak height tends to diverge. These results are consistent with the simulations and analysis results described in the next section.

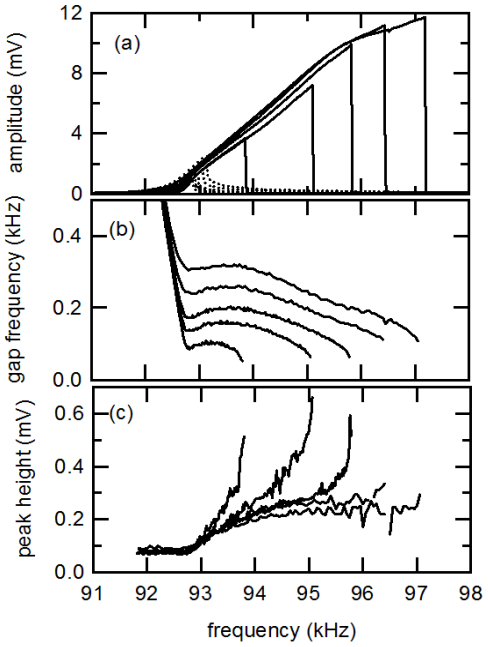

Fig. 4. (a) Cantilever amplitude vs pump frequency for various excitation levels of the pump: 0.14, 0.27, 0.41, 0.68 and 1.0V. Solid and dashed curves are for up-scan and down-scan respectively. (b) Gap frequency between the NF and the pump vs pump frequency for the same pump excitation levels. (c) Peak height of the sideband response vs pump frequency for the different pump levels.

3. Simulations and analysis

(a) Single cantilever

For the model equation of the single Duffing oscillator, we have used

$$m\ddot{x} + \frac{m}{\tau}\dot{x} + k_2 x + k_4 x^3 = m\alpha_1 \cos\left(2\pi f_{pump} t\right) + m\alpha_2 \cos\left(2\pi f_{probe} t\right) \quad (1)$$

where m is the mass, τ is the relaxation time, k_2 and k_4 are harmonic and quartic spring constants, α_1 and α_2 are the driving acceleration amplitude for the pump and probe, and f_{pump} and f_{probe} are the pump and probe frequency, respectively. Values are $m = 1.0\times10^{-10}/(2\pi)^2\,\text{kg}$, $\tau = 0.01s$, $k_2 = 1.0N/m$ and $k_4 = 5.0\times10^8 N/m^3$ throughout the paper.

For the probe, we have used typically $\alpha_2 = 0.01(m/s^2)$. To eliminate the large amplitude vibration oscillating at the pump frequency, we made two sets of simulations with opposite probe phase keeping the pump amplitude fixed. The difference between the two simulations contains only the effect of the probe. Then, the resulting displacement is multiplied by $\cos(2\pi f_{probe} t)$ or $\sin(2\pi f_{probe} t)$ and averaged over a certain time, like a lock-in amplifier, to obtain cosine and sine parts of the probe response. By changing the probe frequency, real and imaginary parts of the response spectra are calculated.

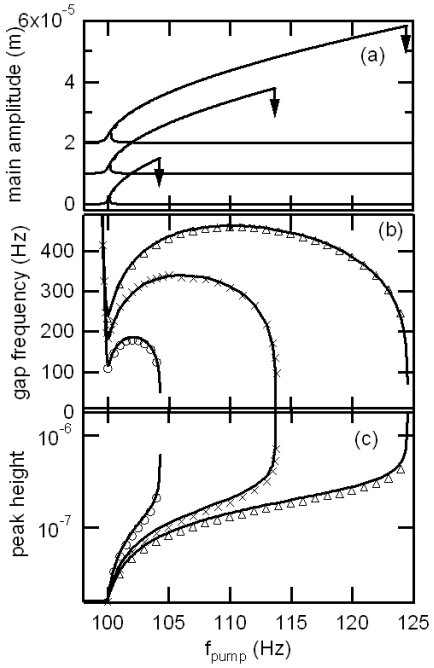

Fig. 5. (a) Nonlinear amplitude response of a single Duffing resonator vs pump frequency. Three pump amplitudes are shown: $\alpha = 1000$, 2000, and 3000 (m/s^2) . (b) Analytically determined sideband gap frequency (solid curves) and simulated peak heights (markers) vs pump frequency. Notation: $\alpha = 1000$ (circles), 2000 (crosses), and 3000 (m/s^2) (triangles). (c) Analytical sideband peak height (solid curve) and simulated gap frequency (markers) vs pump frequency.

Figure 5 summarize the pump frequency dynamics of the Duffing resonator for three different pump excitation levels. Curves in Fig. 5 (a) represent the analytical pump response solutions. Markers in Fig. 5(b) identify the frequency difference of the NF peak and the pump frequency, as a function of the pump frequency. The linear resonance frequency is 100 kHz. The gap frequency increases with the pump frequency from the linear resonance frequency, then decreases beyond the middle of the high amplitude frequency region. It approaches zero as the pump frequency reaches the upper bifurcation frequency. The peak height in Fig. 5(c) increases with increasing pump frequency, and diverging near the upper bifurcation frequency.

The analytical curve was obtained as follows: [7]

$$\tilde{\chi}_a = \frac{\tilde{\chi}_0(\omega)}{1 - \frac{9}{16}\varepsilon^2 \left|\tilde{A}\right|^4 \tilde{\chi}_0(\omega)\tilde{\chi}_0^{\,*}(\omega')} \quad (2)$$

where $\tilde{\chi}_0(\omega) = \dfrac{1}{\omega_{nl}^2 - \omega^2 + i\gamma\omega}$ and $\omega_{nl}^2 = \omega_0^2 + \dfrac{3}{2}\varepsilon\left|\tilde{A}\right|^2$.

Similar sideband curves were obtained by Dykman et al. [10], who studied the Duffing oscillator as a model of a stochastic resonance. Since noise plays an important role in the stochastic resonance, they calculated the spectral density of vibration analytically (Eq. (19) in Ref. [10]). Because of an approximation, their equation is not as simple as Eq. (2) and their peak prediction is distorted by that assumption. Also the gap frequency is related to the stability of the stationary state. For the Duffing equation, stability can be checked by evaluating the perturbed equations in the stationary state. [11-13]

(b) Cantilever array

The equations of motion for the cantilever array simulations have the form

$$m_i \frac{d^2 x_i}{dt^2} + \frac{m_i}{\tau}\frac{dx_i}{dt} + k_{2Oi}x_i + k_{4O}x_i^3 + \sum_j k_{2I}^{(j)}\left(2x_i - x_{i+j} - x_{i-j}\right)$$
$$+ k_{4I}\left\{\left(x_i - x_{i+1}\right)^3 + \left(x_i - x_{i-1}\right)^3\right\}$$
$$= m_i\alpha_{pump}\cos\Omega t + m_i\alpha_{probe}\cos\omega t \quad (3)$$

where m_i is the mass, τ is the relaxation time, k_{2Oi} and k_{4O} are harmonic and quartic onsite spring constant, $k_{2I}^{(j)}$ is the harmonic spring constant for the intersite connection up to 6-th neighbor, and k_{4I} is the quartic spring constant for the intersite connection. The right hand side is the driving term. Here to match experiment $\alpha_{pump} = 1000\,\mathrm{m/s^2}$ is the pump acceleration and Ω is the pump frequency. The second term is for the probe driver at frequency ω and acceleration amplitude $\alpha_{probe} = 0.01\mathrm{m/s^2}$. In the cantilever array, it is observed that the driven ILM displays an amplitude dependence vs pump frequency similar to the Duffing, and bifurcation at a high frequency brings its sudden collapse. [7, 14] We have observed very similar pump frequency dependences of the NF shift and peak height as shown in Figs. 4(b) and (c). Frequency softening and amplitude diverging for these cases at the high frequency transition are sign of the approaching saddle-node bifurcation for the driven-damped Duffing-like response.

To compare more precisely the single cantilever and the ILM cases in experiments and in analytical/simulation, we evaluate $f_{gap}{}^4$, because it is known as a predictor of the saddle-node bifurcation for the undamped condition. [12] Four panels as a function of the driver frequency are to be compared in Fig. 6. In this representation, the saddle node bifurcation takes place where the f_{gap} curve approaches zero at the high frequency location. In all four cases the

curves look almost linear near the bifurcation point; however, the experimental curves in (a) and (c) both bend up as the curves move away from that point, while analytical or simulated cases in (b) and (d) bend down.

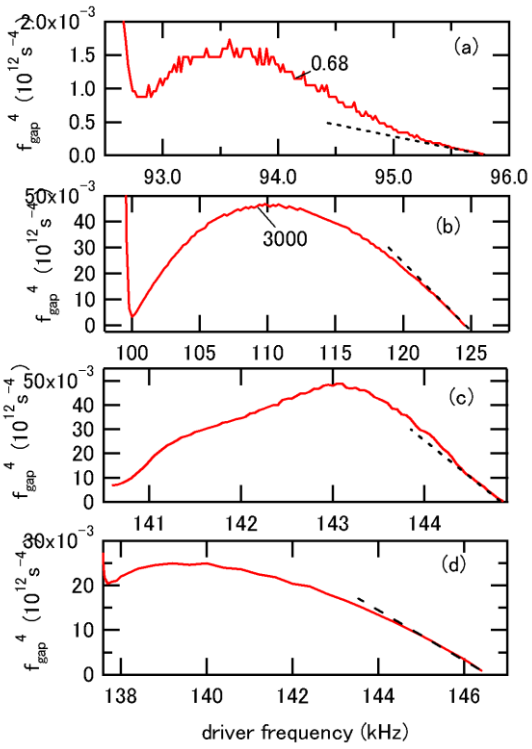

Fig. 6. Predictor of the saddle-node bifurcation, $f_{gap}{}^4$, vs pump frequency for four cases. (a) Experimentally measured single cantilever, (b) Analytically calculated single cantilever, (c) Experimentally measured ILM, and (d) Simulated ILM. (Data from Ref.[7].) The approach to zero on the high frequency side is the signature of the saddle-node bifurcation. Dashed lines are guide to eye.

We might have expected a difference between the single cantilever and ILM cases due to geometry but instead we have found differences between the experimental and analytical/simulated results for both cases. These findings indicate that there is a physical difference between the real cantilever systems and our model equations of motions. A likely candidate is nonlinear damping, with larger damping for the larger amplitude state. In both of the models used, we adopted linear damping with its constant obtained experimentally, but for the small amplitude state.

5. Summary

For the positive nonlinear case studied here, the saddle node bifurcation takes place at the high frequency side of the amplitude spectrum where it drops suddenly as demonstrated in Figs. 4(a) and 5(a). We have found that the measured frequency shift and peak height of the NF resonance for the single cantilever is in good agreement with analytical calculations, as the bifurcation frequency is approached, i.e., the gap frequency decreases and the peak height diverges. We conclude that the analytical linear response equation is valid. The high frequency response of the ILM is comparable to that found for the single cantilever, near the bifurcation point. From both single cantilever and ILM studies, it appears that nonlinear damping in the silicon nitride cantilevers may modify how the NF gap frequency depends on the pump frequency.

Acknowledgments

M. S. was supported by JSPS-Grant-in-Aid for Scientific Research No. 25400394. A. J. S. was supported by Grant NSF-DMR-0906491.

References

[1] E. Kenig, R. Lifshitz, and M. C. Cross, Physical Review E - Statistical, Nonlinear, and Soft Matter Physics **79**, 026203 (2009).

[2] J. F. Rhoads, S. W. Shaw, and K. L. Turner, Journal of Dynamic Systems, Measurement and Control, Transactions of the ASME **132**, 1 (2010).

[3] D. K. Campbell, S. Flach, and Y. S. Kivshar, Physics Today **57**, 43 (2004).

[4] S. Flach and A. V. Gorbach, Physics Reports **467**, 1 (2008).

[5] S. Flach and C. R. Willis, Physical Review Letters **72**, 1777 (1994).

[6] M. Sato, B. E. Hubbard, and A. J. Sievers, Reviews of Modern Physics **78**, 137 (2006).

[7] M. Sato, S. Imai, N. Fujita, W. Shi, Y. Takao, Y. Sada, B. E. Hubbard, B. Ilic, and A. J. Sievers, Physical Review E - Statistical, Nonlinear, and Soft Matter Physics **87**, 012920 (2013).

[8] M. Sato, Y. Sada, W. Shi, S. Shige, T. Ishikawa, Y. Soga, B. E. Hubbard, B. Ilic, and A. J. Sievers, Chaos **25**, 013103 (2014).

[9] V. Hizhnyakov, A. Shelkan, M. Klopov, S. A. Kiselev, and A. J. Sievers, Physical Review B - Condensed Matter and Materials Physics **73**, 224302 (2006).

[10] M. I. Dykman, D. G. Luchinsky, R. Mannella, P. V. E. McClintock, N. D. Stein, and N. G. Stocks, Physical Review E **49**, 1198 (1994).

[11] A. H. Nayfeh and D. T. Mook, *Nonlinear Oscillations* (John Wiley & Sons, New York, 1979).

[12] J. M. T. Thompson and H. B. Stewart, *Nonlinear Dynamics and Chaos* (John Wiley & Sons, Chichester, 1987).

[13] D. W. Jordan and P. Smith, *Nonlinear Ordinary Differential Equations* (Oxford University Press, Oxford, NY, 2007).

[14] M. Sato, S. Imai, N. Fujita, S. Nishimura, Y. Takao, Y. Sada, B. E. Hubbard, B. Ilic, and A. J. Sievers, Physical Review Letters **107**, 234101 (2011).